

See discussions, stats, and author profiles for this publication at: <https://www.researchgate.net/publication/228905182>

X-ray photoelectron spectroscopy of nitromethane adsorption products on Si (100): A model for N 1s core-level shifts in silicon oxynitride films

ARTICLE *in* JOURNAL OF APPLIED PHYSICS · FEBRUARY 2004

Impact Factor: 2.18 · DOI: 10.1063/1.1639951

CITATIONS

24

READS

68

5 AUTHORS, INCLUDING:



R. L. Opila

University of Delaware

213 PUBLICATIONS 4,148 CITATIONS

SEE PROFILE

X-ray photoelectron spectroscopy of nitromethane adsorption products on Si(100): A model for N 1s core-level shifts in silicon oxynitride films

J. Eng, Jr.

Agere Systems, Murray Hill, New Jersey 07974

I. A. Hubner and J. Barriocanal

Department of Chemistry and Biochemistry, University of Delaware, Newark, Delaware 19716

R. L. Opila

Agere Systems, Murray Hill, New Jersey 07974

D. J. Doren^{a)}

Department of Chemistry and Biochemistry, University of Delaware, Newark, Delaware 19716

(Received 11 August 2003; accepted 18 November 2003)

N 1s core-level shifts from x-ray photoelectron spectra (XPS) are reported for the adsorption products of nitromethane (CH_3NO_2) on Si(100). Three spectral peaks are identified and these are associated with specific bonding environments for nitrogen by comparison to predicted core-level shifts from density functional calculations on a range of energetically feasible chemical structures. These species can be classified according to the number of N—O bonds (zero, one, or two) that they contain and, in this sense, they are comparable to the species believed to exist in oxynitride films on Si. Since the energetically feasible products of room-temperature CH_3NO_2 adsorption can be identified with more confidence than those resulting from ion bombardment and high-temperature processing in oxynitride films, nitromethane provides a model system that can aid in correlating spectral features with specific atomic-scale structures. This work supports an earlier proposal that the XPS peak of weakest binding energy is due to species with a dangling bond on nitrogen, while the most intense peak is due to the energetically preferred NSi_3 species. © 2004 American Institute of Physics. [DOI: 10.1063/1.1639951]

I. INTRODUCTION

In recent years, there has been considerable effort in the microelectronics industry to use silicon oxynitrides as an alternative gate dielectric material to replace ultrathin (i.e., <30 Å) silicon dioxide films in complementary metal–oxide–semiconductor devices.¹ This effort has been motivated by the superior electrical and physical properties of silicon oxynitrides, including reduced leakage current,² increased immunity to hot carrier damage,³ and better resistance to boron migration from the p^+ -crystalline Si gate electrode into the channel region.⁴ Additionally, the processing of silicon oxynitride films is compatible with conventional silicon process technology, making silicon oxynitrides a more attractive alternative gate dielectric than some other dielectric materials that have been proposed. On the other hand, depending upon processing, the oxynitride films may actually show decreased breakdown, increased traps, and decreased channel mobility.^{2,5}

To optimize the performance of silicon oxynitride films, it is necessary to first understand the structure of the films at the atomic level. Toward this goal, several research groups have employed x-ray photoemission spectroscopy (XPS) to determine the atomic bonding configuration of nitrogen in thin silicon oxynitride films. A survey of the literature reveals that several different N 1s photoemission features can

be obtained, depending on the method used to grow the silicon oxynitride film.^{6–13} This complexity has led to a variety of different, sometimes contradictory, assignment schemes for the N 1s photoemission features. In particular, it is not even clear whether the NSi_3 moiety, which appears at 398.5–398.7 eV in the N 1s spectrum of a thick Si_3N_4 film,^{6,7} is a major component of oxynitrides. For example, in early work by Carr *et al.*,⁸ the main N 1s feature from an N_2O oxide was 0.7 eV higher than expected for NSi_3 . Arguing that the N 1s feature of an NSi_2O moiety would occur 2.5–3.0 eV higher than that of NSi_3 , Carr *et al.*⁸ concluded that their main N 1s feature was attributable to a NSi_2 species, wherein nitrogen was two-fold coordinated with the remaining sp^3 orbital existing as a dangling bond. In a later study by Bhat *et al.*⁹ of N_2O oxides nitrided in NH_3 , the N 1s spectrum of an N_2O oxide reference film exhibited a feature assigned to NSi_3 at 397.6 eV and a second feature with a 2.2 eV higher binding energy, which was assigned to an NSi_2O group. Interestingly, one spectrum in their NH_3 nitrided N_2O oxide study, recorded at shallow photoelectron take-off angle to enhance the sensitivity to the near-surface region, showed an additional distinct feature at ~ 402 eV. This feature was not assigned. Hedge *et al.*¹⁰ observed N 1s features at 397.99 and 400.99 eV after using NO to add nitrogen to thermal oxides, and assigned these features to NSi_3 and NSi_2O . In contrast to all of the studies described so far, where the binding energy difference between NSi_3 and NSi_2O is at least 2.0 eV, studies by Lu *et al.*¹¹ suggested a much smaller separa-

^{a)}Electronic mail: doren@udel.edu

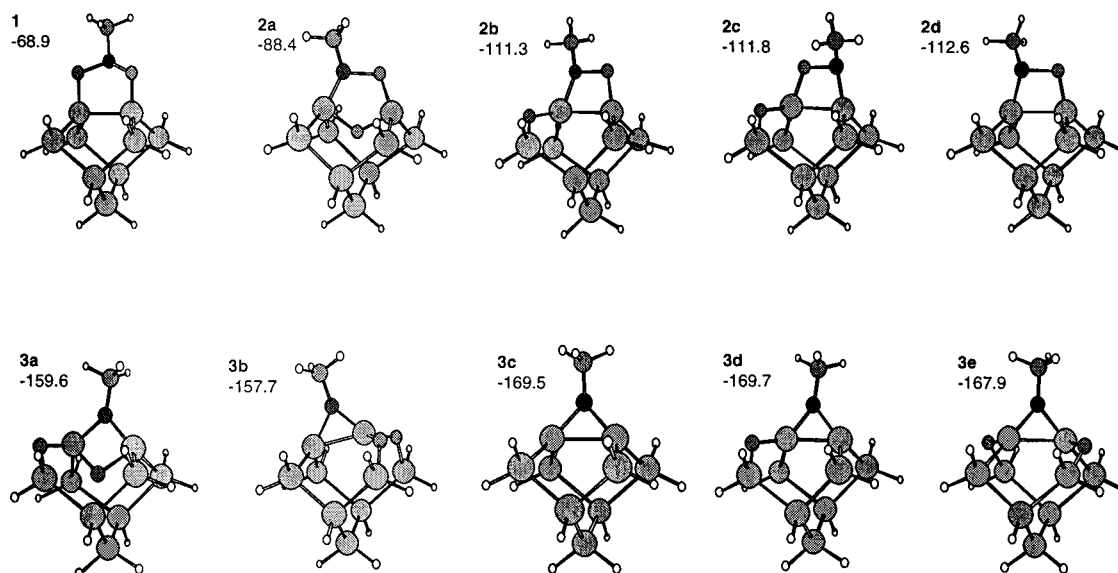


FIG. 1. Initial cycloaddition product of CH_3NO_2 , **1**, and some possible rearrangement products. **1** is the only species in which nitrogen is bound to two oxygen molecules. Species **2a–d** all have nitrogen bound to one oxygen and one Si. In structures **3a–e**, nitrogen has no bonds to oxygen. Structures are determined using B3LYP/6-31G(d). For each structure, the energy is given relative to separated CH_3NO_2 and the cluster model (energy in kcal/mol, calculated with B3LYP/6-311++G(2df,2p), not including zero-point energy). The alphabetic ordering within groupings is based on the relative magnitude of the N 1s binding energy in the effective core approximation (Table II).

tion of 0.85 eV between the N 1s features of NSi_3 and NSi_2O . Other studies by Shallenberger *et al.*¹² found that the N 1s binding energy shift of NSi_2O was 1.6–2.2 eV greater than that of NSi_3 . They also observed a third feature at 402.8 eV, which they attributed to an NSiO_2 structure.

In a study by Chang *et al.*,¹³ the structure of silicon oxynitrides prepared by a combination of thermal oxynitridation and low-energy nitrogen ion implantation was studied using angle-resolved x-ray photoemission, in conjunction with analysis by the maximum entropy method. In that study, N 1s features were observed at 397.5, 399.2, 401.2, and 403.6 eV and were assigned tentatively to NSi_3 , NOSi_2 , NO_2Si , and NO_3 , respectively. This assignment was based upon the observation that the approximately even spacing between peaks (~ 1.8 eV) matches the spacing for the NSi_3 , NOSi_2 , NO_2Si , and NO_3 predicted by the density functional theory (DFT) calculations of Rignanese *et al.*¹⁴ on model molecules and films. However, basing the assignments strictly on peak spacing led Chang *et al.*¹³ to assign the most intense feature in their spectrum to an NOSi_2 moiety, and a minor peak to NSi_3 . This conclusion was tentative, because N—O bonds are known to be much weaker than Si—O bonds, implying that NOSi_2 species will be thermodynamically unstable relative to NSi_3 and SiO_x . As a result, these authors noted that other species with dangling bonds or positively charged, overcoordinated nitrogen defect centers that had not been treated theoretically might also contribute to the spectrum.

To address the uncertainty in assigning the N 1s spectra of silicon oxynitrides, Rignanese and Pasquarello performed a comprehensive set of calculations using DFT to determine the N 1s core-level shifts for nitrogen in a variety of bonding configurations.¹⁵ All nearest-neighbor oxygen configurations $\text{NO}_x\text{Si}_{3-x}$ (where $0 < x < 3$) were considered, as well as situ-

ations where a nitrogen atom is bonded to two silicon atoms, but possesses a dangling bond that can be full, empty, or partially occupied. These calculations also examined the contribution of final state effects to the binding energy shift of N 1s core levels. Rignanese and Pasquarello showed that the alternative interpretation of the XPS spectra of Chang *et al.*,¹³ in which the most intense peak was due to NSi_3 , while the minor peak at lowest binding energy was due to N species with a dangling bond, was consistent with the observed peak spacing. This is in many ways a more satisfying interpretation than the one that assigns the small peak at the lowest binding energy to NSi_3 , but there is no published experimental evidence for the presence of a dangling bond species.¹⁶

Although all of these studies have added to the overall understanding of nitrogen in silicon oxynitride films, a conspicuous lack of any experimental standards for assigning the N 1s spectra of silicon oxynitride films has remained. In this article, we use a combination of XPS and DFT to demonstrate that the reaction of the Si(100) surface with nitromethane (CH_3NO_2) can be used as a model system to provide an experimental basis for assigning these N 1s spectra. This work is motivated by earlier DFT studies by Barriocanal and Doren,¹⁷ who showed that the reaction products of CH_3NO_2 with the Si(100) surface are likely to include several bonding environments around nitrogen, with varying numbers of bonds to oxygen and silicon. Specifically, the initial product (**1**, Fig. 1) is predicted to form with no activation barrier. However, this initial product is thermodynamically unstable with respect to rearrangement products that have fewer N—O bonds and more Si—O bonds. Examples of such products are shown in Fig. 1, with additional possibilities described in Ref. 17. The CH_3NO_2 surface reaction products can be classified into three categories: (1)

The initially adsorbed species containing two N—O bonds (NO_2C), (2) products **2a–d**, which contain just one N—O bond (NOSiC); and (3) products **3a–e**, containing no N—O bonds (NSi_2C). Given the chemical similarity of Si and C, this mixture of products may serve as a model system for understanding the photoemission spectra of silicon oxynitride films. Compared to oxynitride films produced with ion bombardment, there are relatively few possible configurations in a film produced by molecular adsorption from a thermal gas. Here, we show that electronic structure calculations can be used to correlate the structures of Fig. 1 with N $1s$ core-level shifts in the products of CH_3NO_2 adsorption on Si, and in turn assign the observed core-level shifts in oxynitride films to particular bonding environments for nitrogen.

II. EXPERIMENT

A. X-ray photoemission spectroscopy and sample preparation

The x-ray photoemission experiments were performed on a Physical Electronics (Chanhassen, MN) Model 5600 x-ray photoelectron spectrometer, which is equipped with a monochromated Al K x-ray source and a hemispherical analyzer. Typically, the spectra were recorded with a pass energy setting of 11.75 eV and a step size of 0.1 eV. To account for slight charging effects, all spectra were shifted to center the C $1s$ peak at 285.0 eV. The sample was oriented such that the photoelectron take-off angle was 45° relative to the surface plane.

The $1\text{ cm} \times 1\text{ cm}$ Si(100) samples used in this study were cleaned and hydrogen terminated using the following three step process: (1) Degreasing sequentially in acetone and methanol, (2) immersion in a 1:1:4 $\text{NH}_4\text{OH}/\text{H}_2\text{O}_2/\text{H}_2\text{O}$ solution at 80°C followed by a 1:1:4 $\text{HCl}/\text{H}_2\text{O}_2/\text{H}_2\text{O}$ solution at 80°C , and (3) immersion in concentrated hydrofluoric acid. After wet chemical processing, the Si samples were immediately transferred to the load lock of the XPS chamber, pumped to $<10^{-7}$ Torr, and inserted into the XPS analysis chamber (base pressure 1×10^{-10} Torr). To generate a clean Si(100)- 2×1 surface, the Si samples were heated to 560°C , and cooled to room temperature with the assistance of a liquid-nitrogen-cooled copper braid in contact with the sample mount. CH_3NO_2 [Aldrich, St. Louis, MO, 99+ % purity] was purified by successive freeze–pump–thaw cycles prior to being admitted to the chamber via a leak valve. All exposures were made at -50°C .

B. Theoretical methods

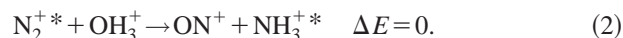
Calculations have been performed using the B3LYP hybrid density functional,^{18,19} with 6-31G(d) and 6-311G(2df,2p) basis sets, as implemented in GAUSSIAN98.²⁰ A Si_9H_{12} cluster is used to model the surface with subsurface bonds constrained to prevent unrealistic distortions, as described in Ref. 17. The geometry of each molecule was optimized with the smaller basis set, and single point energy calculations were done with the larger basis set. According to Koopman's theorem (KT), the orbital energy of the nitrogen $1s$ electron approximates the core-level binding energy,

though this neglects any relaxation of the other orbitals in response to the ionization. Relaxation effects are difficult to obtain by direct calculation because the highly excited core hole states are not amenable to standard variational methods. An estimate of core-level shifts that accounts for relaxation of the valence electrons in the final state can be obtained using the equivalent core [(EC) or $Z+1$] approximation. This approach models an atomic core lacking one electron by the filled core of the next element ($Z+1$) in the periodic table. The EC approximation has been widely used to determine and systematize chemical shifts in photoelectron spectra.²¹

The EC approximation obtains the chemical shift in a core electron binding energy as the energy of a hypothetical chemical reaction. For example, the difference between the N $1s$ binding energies in ammonia and nitrogen molecules, ΔE_B , is the reaction energy of



where an asterisk designates a N $1s$ hole. The EC allows calculations on ground-state species by assuming that the energy is not changed if both +6 nitrogen cores (corresponding to the core with a N $1s$ hole) are replaced by a +6 oxygen core (with no hole), i.e.,



Adding reactions (1) and (2) yields



which allows calculation of ΔE_B from ground-state energies only. The EC approximation holds that the interchange of equally charged cores is isoenergetic. This does not require that the cores are chemically equivalent. Rather, it is only necessary that all core replacements for a particular element have the same energy change, so that the difference for any pair of replacements is zero.²¹ Note that this method produces binding energy shifts, not absolute binding energies. Moreover, while it accounts for final state effects due to relaxation of valence electronic states and polarization within the cluster model, it does not include the long-range electrostatic screening due to the presence of the extended substrate that may be observed in experiments. For this model system, the distance of nitrogen from the surface is similar in all the models, so screening effects are not likely to account for significant variation, but we will address this point again in analyzing the experimental results.

III. RESULTS AND DISCUSSION

A. Equivalent core method calculations

To test the EC approximation, calculated N $1s$ binding energies were compared with experimentally derived values tabulated by Jolly²² (Table I). NH_3 was used as a reference for this calibration because it has an sp^3 valence configuration similar to the CH_3NO_2 adducts, and there is little uncertainty in its measured core electron binding energy. The difference in relative binding energies as predicted with the KT and EC approximations (Table I) shows that final state effects can be substantial (0.1–0.8 eV) in this set of molecules.

TABLE I. N $1s$ binding energies relative to NH_3 , in eV; positive values indicate a shift to higher binding energy. The average of measured values from Ref. 22 is given, with standard deviations (σ) where more than one measurement is available. Calculated values from KT and the EC method are given along with the deviation from the averaged measured value and the mean absolute deviation (MAD) for each approximation method. Energies were calculated using B3LYP/6-311++G(2df,2p) at geometries obtained with B3LYP/6-31G(d).

Molecule	Measured ΔE_B (eV)		Predicted ΔE_B (eV)			
	Average	σ	KT	Deviation	EC	Deviation
N_2	4.25	0.20	3.47	-0.78	3.65	-0.60
NH_3	0.00	0.05	0.00	0.00	0.00	0.00
NO_2	7.18	0.21	7.50	0.32	7.21	0.03
NH_2CH_3	-0.43	0.04	-0.07	0.36	-0.53	-0.10
$\text{NH}(\text{CH}_3)_2$	-0.66	0.02	0.08	0.74	-0.79	-0.13
$\text{N}(\text{CH}_3)_3$	-0.76	0.01	0.28	1.04	-0.97	-0.21
NO	4.91	0.33	4.53	-0.38	4.63	-0.28
$\text{N}_2\text{O}(\text{NN}^*\text{O})$	6.99	0.08	6.93	-0.06	7.02	0.03
$\text{N}_2\text{O}(\text{N}^*\text{NO})$	3.08	0.13	3.42	0.34	2.53	-0.55
HCN	0.79	0.38	1.33	0.54	0.59	-0.20
NO_2CH_3	5.59	N/A ^a	7.29	1.70	6.63	1.04
MAD (eV)				0.63		0.32

^aNot applicable.

EC predictions are (with only one exception) in much better agreement with the experiment than KT predictions. The orbital eigenvalues show a small but significant dependence on the basis set, but this effect is even smaller in the EC approximation. Within the EC approximation, the mean absolute deviation between predicted and measured values is only 0.3 eV; the largest deviations are for CH_3NO_2 , N_2 , and N_2O , though the electronic structures of these molecules are very different than those of the surface adducts. Among molecules with three single bonds to nitrogen (as is the case with the surface adducts), the deviation is never more than 0.25 eV. The accuracy of the EC predictions is comparable to that obtained by Rignanese *et al.*¹⁴ using somewhat different methods.

Calculated core-level shifts for the nitromethane adducts are shown in Table II. The rearranged CH_3NO_2 adduct with no oxygen neighbors, **3c**, is used as the reference. The core-level peaks fall into three well-separated clusters, according

TABLE II. N $1s$ core-level shifts (in eV) for the species of Fig. 1, relative to the initial cycladdition product, **1**. Values were obtained from KT and the EC approximations, using B3LYP/6-311++G(2df,2p)//B3LYP/6-31G(d) energies.

Surface adduct	Predicted ΔE_B (eV)	
	KT	EC
1	3.25	3.21
2a	1.55	1.57
2b	1.22	1.37
2c	1.31	1.29
2d	1.23	1.23
3a	0.03	0.16
3b	0.08	0.00
3c	0.00	0.00
3d	0.03	-0.05
3e	0.09	-0.09

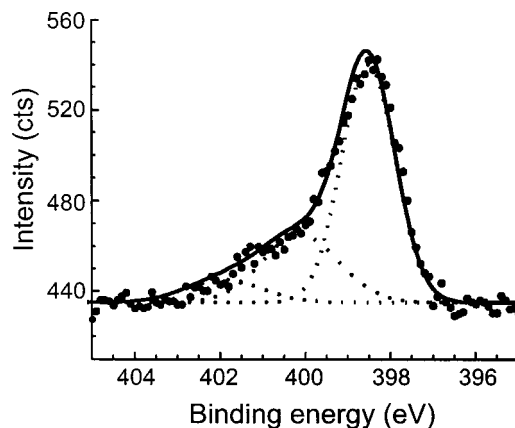


FIG. 2. X-ray photoelectron spectrum of N $1s$ of 540 L of CH_3NO_2 adsorbed on Si(100). Shown in addition to the data are the individual components plus the Shirley baseline (dot) and the total fit plus baseline (solid).

to the number of oxygens bound to nitrogen. The initial adduct **1**, with two N—O bonds (NO_2C), has the most positive binding energy, shifted by 3.25 eV from the reference. The N $1s$ core levels of the family of structures **2a–d**, with a single N—O bond (NOSiC), are shifted by 1.23 to 1.57 eV. For the family **3a–e**, with no N—O bonds (NSi_2C), the core-level shifts are small, falling into the range -0.09 to 0.16 eV. While the main contribution to the core-level shift is the number of bonds to oxygen, the range of values within each family is due to differences in ring strain and second neighbors. For example, the species with oxygen inserted in the dimer bond, **2a** and **3a**, have a N $1s$ binding energy 0.2–0.3 eV greater than the other structures with the same number of N—O bonds. On the other hand, the dependence on second neighbors is not easily described. In both structures **3b** and **3e**, nitrogen has two second-neighbor oxygens, yet their binding energies bracket that of structure **3d**, which has only one oxygen second neighbor. Clearly, the effect of second neighbors on core-level shifts depends as much on details of structure as it does on the number of second neighbors.

B. X-ray photoemission spectroscopy study

Figure 2 shows a N $1s$ spectrum recorded after exposing a clean Si(100) surface at -50°C to 540 L of CH_3NO_2 . The raw spectrum shows a single asymmetric peak with a pronounced shoulder at higher binding energy. To determine the contributions to this feature, it was decomposed using a Shirley background, three 80% Gaussian-20% Lorentzian curves with a full width at half maximum of 1.6 eV. Note that three curves were necessary to obtain a good fit. With only two curves of approximately equal width, it is impossible to reproduce the shape of the spectrum, with particularly bad agreement on the high binding energy side of the N $1s$ feature.

The three main N $1s$ features appear at 398.5, 400.1, and 401.9 eV. As described above, the possible rearrangement products for CH_3NO_2 on Si(100) can be categorized by the number of N—O bonds. Using this as a qualitative basis for assignments, the highest binding energy feature at 401.9 eV

is attributed to the molecularly adsorbed CH_3NO_2 because the nitrogen atom is attached to the largest possible number of electron-withdrawing oxygen atoms. Applying similar reasoning, the middle feature at 400.1 eV is assigned to rearrangement products that have just one N—O bond, and the lowest binding energy feature at 398.9 eV is assigned to rearrangement products where no oxygen atoms are directly attached to the nitrogen atom. It should be noted that the relative intensities of these features in Fig. 2 indicate that molecularly adsorbed CH_3NO_2 is a minority species on the surface; the Si(100) surface is covered predominantly with rearrangement products where the N—O bonds have broken and the oxygen atoms have inserted into Si backbonds. This interpretation assigns the largest peak to the most energetically stable class of species. However, the product distribution is far from the thermodynamic distribution: The large difference in relative energies of the species in Fig. 1 shows that only the species without N—O bonds could be present in significant amounts at equilibrium. A comparison of the experimentally observed N 1s features with those calculated using the EC approximation shows good agreement in the relative spacing between the N 1s features, though the calculations are not designed to calculate absolute binding energy shifts. For example, using the binding energy of the feature assigned to the species with no N—O bonds (centered at 398.5 eV) as a reference, the experimental feature assigned to products with just one N—O bond (centered at 400.1 eV) occurs at 1.6 eV higher binding energy. This may be compared to the EC prediction of shifts of 1.23 to 1.57 eV for the calculated structures with a single N—O bond. The feature assigned to the initial adduct (centered at 401.9 eV) is shifted by 3.4 eV, relative to the reference peak. Again, the shift predicted by EC, 3.2 eV, is in very good agreement with the proposed assignment. Note that the range of binding energies calculated for each class of structures is much smaller than the width of the experimental features, so there is no prospect of making assignments to specific structures within each group. There is also no evidence for different contributions in electrostatic screening of the final state for different species (not fully accounted for in the EC approximation).

C. Comparison to previous studies

The experiments by Chang *et al.*¹³ on an oxynitride film showed both a wider range of binding energies and somewhat wider spacing between peaks (1.8–2.4 eV) than those observed in the present work (1.6–1.8 eV). The peak spacings observed by Chang *et al.*¹³ appear to be in remarkably close agreement with the calculations of Rignanese *et al.*¹⁴ for some model molecules of the type $(\text{H}_3\text{SiO})_n\text{N}(\text{SiH}_3)_{3-n}$ with $n=0-3$. However, as noted above, this requires assigning the largest peak to an energetically disfavored species. Moreover, when Rignanese *et al.*^{14,15} predicted core-level shifts for more realistic models of oxynitride films, they found smaller peak spacings (1.5–2.0 eV) than in the molecular analogs, implying less precise agreement with the experiments of Chang *et al.*¹³ In order to explain a number of other experiments, Rignanese *et al.*¹⁴ noted that second-neighbor effects (which may include electronic interactions

through space or through bonds, as well as bond strain due to local geometric constraints) could increase the peak spacings and estimated that this effect could shift peaks by as much as 0.36 eV. In fact, they concluded that the major N 1s peak in oxynitrides was due to NSi_3 , in contrast to the preliminary assignment of Chang *et al.*¹³

The calculated peak spacings in the present work are quite close to those calculated by Rignanese *et al.*¹⁴ for N atoms in their models of oxynitride films. We can compare our calculations to theirs by treating species with the same number of N—O bonds as equivalent. That is, we compare our calculated core shifts for $\text{N-CSi}_x\text{O}_{2-x}$ ($x=0-2$) structures to their core shifts for $\text{N-Si}_{x+1}\text{O}_{2-x}$ ($x=0-2$) in film models. Taking **3c** (with no N—O bonds) as the reference, we predict the shift due to replacement of one N—Si bond by a N—O bond will be 1.23 to 1.57 eV, while Rignanese *et al.*¹⁴ predict a shift of 1.5 eV. We calculate the total shift for systems with both N—Si bonds replaced by N—O bonds is 3.21 eV, while they find it to be 3.5 eV. Given the differences in geometry and composition, the agreement between the present calculations on adsorption products of CH_3NO_2 and the earlier work on the Si-oxynitride interface model is remarkable. Thus, analysis of the CH_3NO_2 products provides a model of the species in an oxynitride film, which does not require accounting for variations in composition, electrostatics, and escape probability across the film thickness.

In our assignment of the XPS spectrum for CH_3NO_2 adsorption products, the major peak (398.5 eV) corresponds to NSi_2C species. This is consistent with the expectation from thick Si_3N_4 films, where the observed N 1s peak (due to NSi_3) is at 398.6 eV. It is, however, 0.7 eV lower in binding energy than the major peak in the oxynitride film studied by Chang *et al.*,¹³ supporting the notion that the NSi_3 peak in the oxynitride is shifted to higher binding energy by second neighbors (though we cannot rule out effects of differences in strain among these systems). The remaining peaks in the CH_3NO_2 spectrum at higher binding energy are assigned to the NOSiC and NO_2C species. With this assignment, the spacing between these peaks agrees with our calculations and with those of Rignanese *et al.*,¹⁴ but is smaller than that in the oxynitride films of Chang *et al.*¹³ Again, this may reflect second-neighbor effects (or strain) in the film, that are different from those in the CH_3NO_2 products and theoretical models.

While the peaks observed in oxynitride films have different absolute energies than the CH_3NO_2 products, this is reasonably attributed to the effects of film thickness and second neighbors. Thus, we propose that the largest peak observed by Chang *et al.*¹³ in the oxynitride film (centered at 399.2 eV) should be assigned to NSi_3 , while the higher binding energy peaks correspond to NOSi_2 and NO_2Si . This interpretation assigns the largest peak in the spectra for the oxynitride to the most stable bonding configuration. This peak assignment is consistent with one proposed by Rignanese and Pasquarello,¹⁵ in which the peak at weakest binding energy is due to a dangling bond species and the most intense peak is due to NSi_3 . In the oxynitride, there is no direct evidence to distinguish that assignment from the alternative proposal that the weakest binding energy peak is due

to NSi_3 . The evidence presented here for CH_3NO_2 adsorption products supports the proposal of Rignanese and Pasquarello¹⁵ with evidence from a system with a relatively small number of energetically feasible structures.

IV. CONCLUSIONS

Adsorption of CH_3NO_2 on Si(100) produces an array of products that mimic the chemical species observed in silicon oxynitride films. The N $1s$ spectra of the CH_3NO_2 products can be assigned with a high degree of certainty because there are relatively few chemically reasonable structures for CH_3NO_2 products and these can be readily treated with accurate theoretical methods. This model system provides evidence for an interpretation of the spectra of oxynitride films that assigns the most intense peak to the thermally stable NSi_3 species.

ACKNOWLEDGMENT

Part of this material is based upon work supported by the National Science Foundation under Grant No. 9971241.

¹M. L. Green, E. P. Gusev, R. Degraeve, and E. L. Garfunkel, *J. Appl. Phys.* **90**, 2057 (2001).

²E. P. Gusev, D. A. Buchanan, P. Jamison, T. H. Zabel, and M. Copel, *Microelectron. Eng.* **48**, 67 (1999).

³T. Hori and H. Iwasaki, *IEEE Electron Device Lett.* **10**, 64 (1989).

⁴C. H. Chen, Y. K. Fang, and C. W. Yang, *IEEE Electron Device Lett.* **22**, 378 (2001).

⁵R. Perara, A. Ikeda, R. Hattori, and Y. Kuroki, *Thin Solid Films* **423**, 212 (2003).

⁶G. M. Ingo and N. Zacchetti, *High. Temp. Sci.* **28**, 137 (1990).

⁷M. S. Donley, D. R. Baer, and T. G. Stobe, *Surf. Interface Anal.* **11**, 335 (1988).

⁸E. C. Carr, K. A. Ellis, and R. A. Buhrman, *Appl. Phys. Lett.* **66**, 1492 (1995).

⁹M. Bhat, J. Ahn, D. L. Kwong, M. Arendt, and J. M. White, *Appl. Phys. Lett.* **64**, 1168 (1994).

¹⁰R. I. Hedge, P. J. Tobin, K. G. Reid, B. Maiti, and S. A. Ajuria, *Appl. Phys. Lett.* **66**, 2882 (1995).

¹¹Z. H. Lu, R. J. Hussey, M. J. Graham, R. Cao, and S. P. Tay, *J. Vac. Sci. Technol. B* **14**, 2882 (1996).

¹²J. Shallenberger, D. Cole, and S. Novak, *J. Vac. Sci. Technol. A* **17**, 1086 (1999).

¹³J. P. Chang, M. L. Green, V. M. Donnelly, R. L. Opila, J. Eng, Jr., J. Sapjeta, P. J. Silverman, B. Weir, H. C. Lu, T. Gustafsson, and E. Garfunkel, *J. Appl. Phys.* **87**, 4449 (2000).

¹⁴G.-M. Rignanese, A. Pasquarello, J.-C. Charlier, X. Gonze, and R. Car, *Phys. Rev. Lett.* **79**, 5174 (1997).

¹⁵G.-M. Rignanese and A. Pasquarello, *Phys. Rev. B* **63**, 075307 (2001).

¹⁶Opila and Eng (unpublished) have reported electron spin resonance and near-edge x-ray absorption data consistent with the presence of unsatisfied, dangling bonds in specimens with the low binding energy N $1s$ photoemission.

¹⁷J. A. Barriocanal and D. J. Doren, *J. Phys. Chem.* **104**, 12269 (2000).

¹⁸A. D. Becke, *J. Chem. Phys.* **98**, 1372 (1993).

¹⁹C. Lee, W. Yang, and R. G. Parr, *Phys. Rev. B* **37**, 785 (1988).

²⁰M. J. Frisch *et al.*, GAUSSIAN98, Revision A.7, (Gaussian, Inc., Pittsburgh, PA, 1998).

²¹W. L. Jolly, in *X-Ray Photoelectron Spectroscopy*, edited by T. A. Carlson (Academic, New York, 1978).

²²W. L. Jolly *et al.*, *At. Data Nucl. Data Tables* **31**, 433 (1984).

Journal of Applied Physics is copyrighted by the American Institute of Physics (AIP). Redistribution of journal material is subject to the AIP online journal license and/or AIP copyright. For more information, see <http://ojps.aip.org/japo/japcr/jsp>
Copyright of Journal of Applied Physics is the property of American Institute of Physics and its content may not be copied or emailed to multiple sites or posted to a listserv without the copyright holder's express written permission. However, users may print, download, or email articles for individual use.